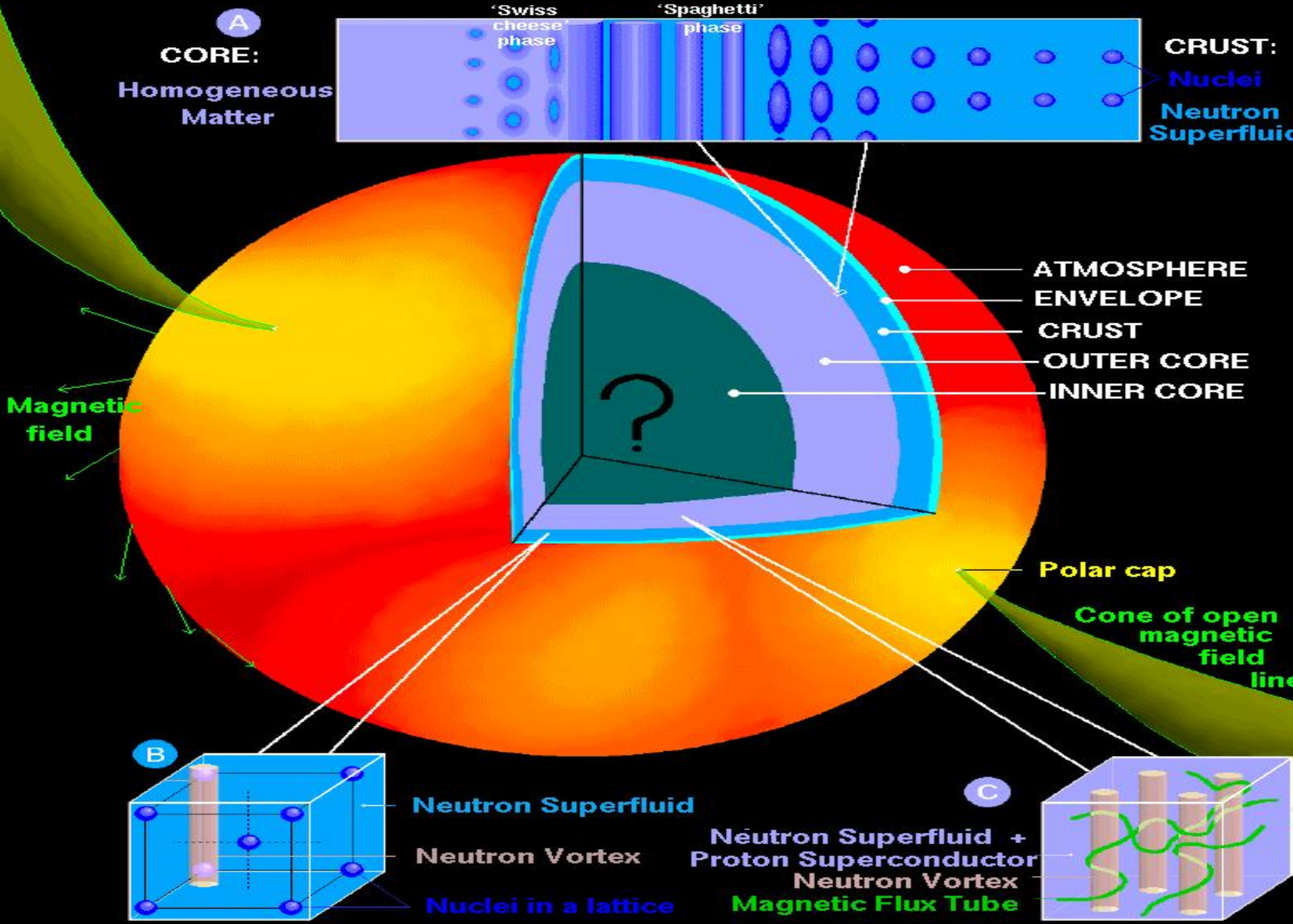


# Magnetar Oscillations: Shedding Light on the Neutron Star Equation of State

Stephen R. Schwartz

# A NEUTRON STAR: SURFACE and INTERIOR



# State of Nuclei Below Neutron Drip

EQUILIBRIUM NUCLEI BELOW NEUTRON DRIP

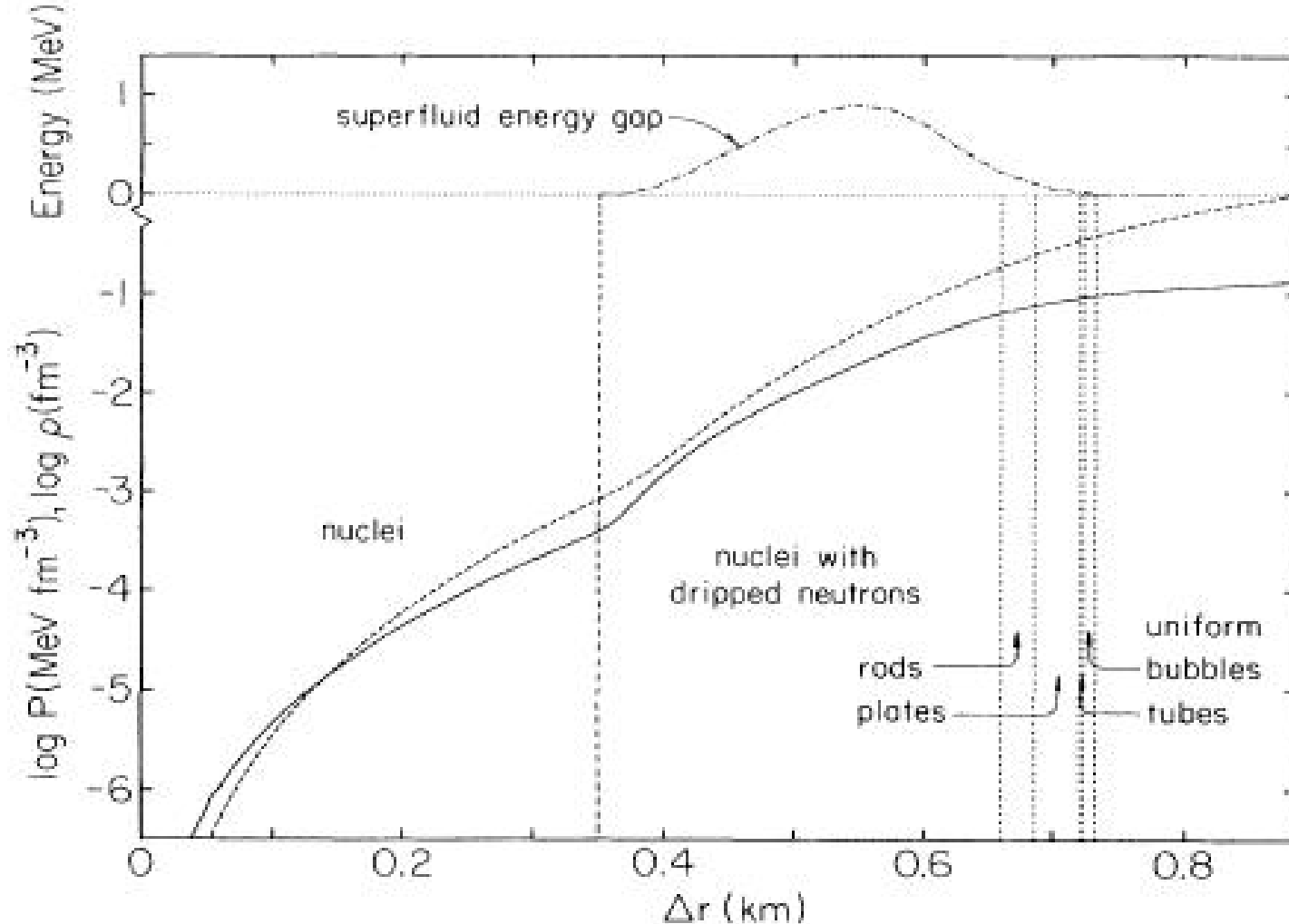
| Nucleus                 | $b$<br>(MeV) | $Z/A$  | $\rho_{\max}$<br>( g cm $^{-3}$ ) | $\mu_e$<br>(MeV) | $\Delta\rho/\rho$<br>(%) |
|-------------------------|--------------|--------|-----------------------------------|------------------|--------------------------|
| $^{56}\text{Fe}$ .....  | 8.7905       | 0.4643 | $8.1 \times 10^6$                 | 0.95             | 2.9                      |
| $^{62}\text{Ni}$ .....  | 8.7947       | 0.4516 | $2.7 \times 10^8$                 | 2.6              | 3.1                      |
| $^{64}\text{Ni}$ .....  | 8.7777       | 0.4375 | $1.2 \times 10^9$                 | 4.2              | 7.9                      |
| $^{84}\text{Se}$ .....  | 8.6797       | 0.4048 | $8.2 \times 10^9$                 | 7.7              | 3.5                      |
| $^{82}\text{Ge}$ .....  | 8.5964       | 0.3902 | $2.2 \times 10^{10}$              | 10.6             | 3.8                      |
| $^{80}\text{Zn}$ .....  | 8.4675       | 0.3750 | $4.8 \times 10^{10}$              | 13.6             | 4.1                      |
| $^{78}\text{Ni}$ .....  | 8.2873       | 0.3590 | $1.6 \times 10^{11}$              | 20.0             | 4.6                      |
| $^{76}\text{Fe}$ .....  | 7.9967       | 0.3421 | $1.8 \times 10^{11}$              | 20.2             | 2.2                      |
| $^{124}\text{Mo}$ ..... | 7.8577       | 0.3387 | $1.9 \times 10^{11}$              | 20.5             | 3.1                      |
| $^{122}\text{Zr}$ ..... | 7.6705       | 0.3279 | $2.7 \times 10^{11}$              | 22.9             | 3.3                      |
| $^{120}\text{Sr}$ ..... | 7.4522       | 0.3166 | $3.7 \times 10^{11}$              | 25.2             | 3.5                      |
| $^{118}\text{Kr}$ ..... | 7.2002       | 0.3051 | $(4.3 \times 10^{11})$            | (26.2)           | ...                      |

NOTE.— $b$  is the binding energy per nucleon;  $\rho_{\max}$  is the maximum density at which the nuclide is present;  $\mu_e$  is the electron chemical potential at that density, and  $\Delta\rho/\rho$  is the fractional increase in the mass density in the transition to the next nuclide. The value of  $\rho_{\max} = 4.3 \times 10^{11}$  g cm $^{-3}$  is the density at which neutron drip begins.

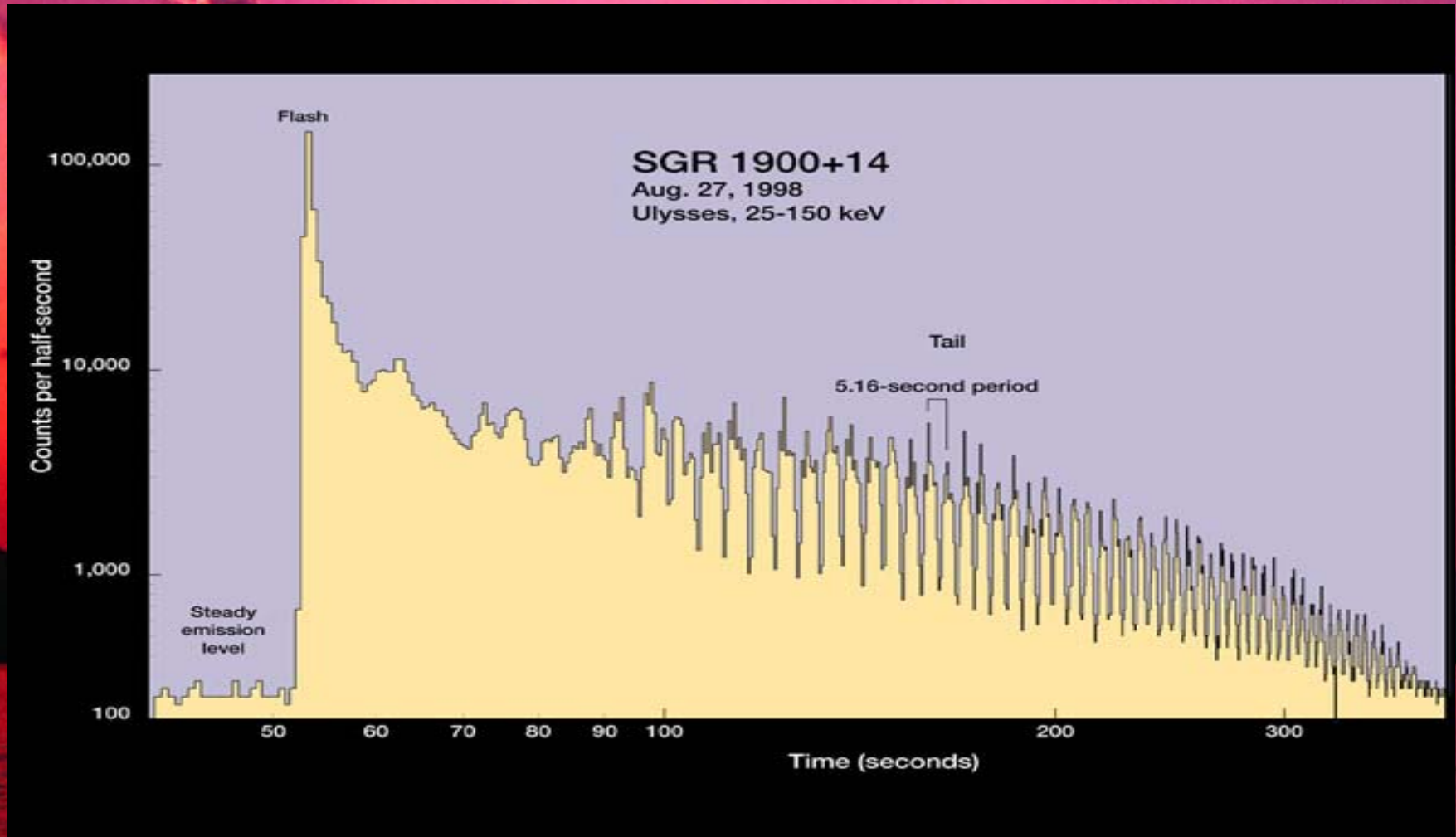
# State of Nuclei Above Neutron Drip

| $\mu_n$ [MeV] | $\mu_p$ [MeV] | $n_b$ [ $\text{cm}^{-3}$ ] | Element            | $Z$ | $N$  |
|---------------|---------------|----------------------------|--------------------|-----|------|
| 0.2           | -26.8         | $2.79 \times 10^{35}$      | $^{180}\text{Zr}$  | 40  | 140  |
| 0.3           | -29.4         | $4 \times 10^{35}$         | $^{200}\text{Zr}$  | 40  | 160  |
| 0.6           | -29.5         | $6 \times 10^{35}$         | $^{250}\text{Zr}$  | 40  | 210  |
| 1.0           | -28.5         | $8.79 \times 10^{35}$      | $^{320}\text{Zr}$  | 40  | 280  |
| 1.4           | -29.4         | $1.59 \times 10^{36}$      | $^{500}\text{Zr}$  | 40  | 460  |
| 2.6           | -33.6         | $3.73 \times 10^{36}$      | $^{950}\text{Sn}$  | 50  | 900  |
| 3.3           | -34.5         | $5.77 \times 10^{36}$      | $^{1100}\text{Sn}$ | 50  | 1050 |
| 4.2           | -35.8         | $8.91 \times 10^{36}$      | $^{1350}\text{Sn}$ | 50  | 1300 |
| 6.5           | -43.6         | $2.04 \times 10^{36}$      | $^{1800}\text{Sn}$ | 50  | 1750 |
| 10.9          | -54.0         | $4.75 \times 10^{37}$      | $^{1500}\text{Zr}$ | 40  | 1460 |
| 15            | -68.3         | $7.89 \times 10^{37}$      | $^{980}\text{Ge}$  | 32  | 950  |

# Nuclear State Within in Neutron Star Crust



# $\gamma$ -ray Light Curve of Magnetar Giant Flare from SGR 1900+14



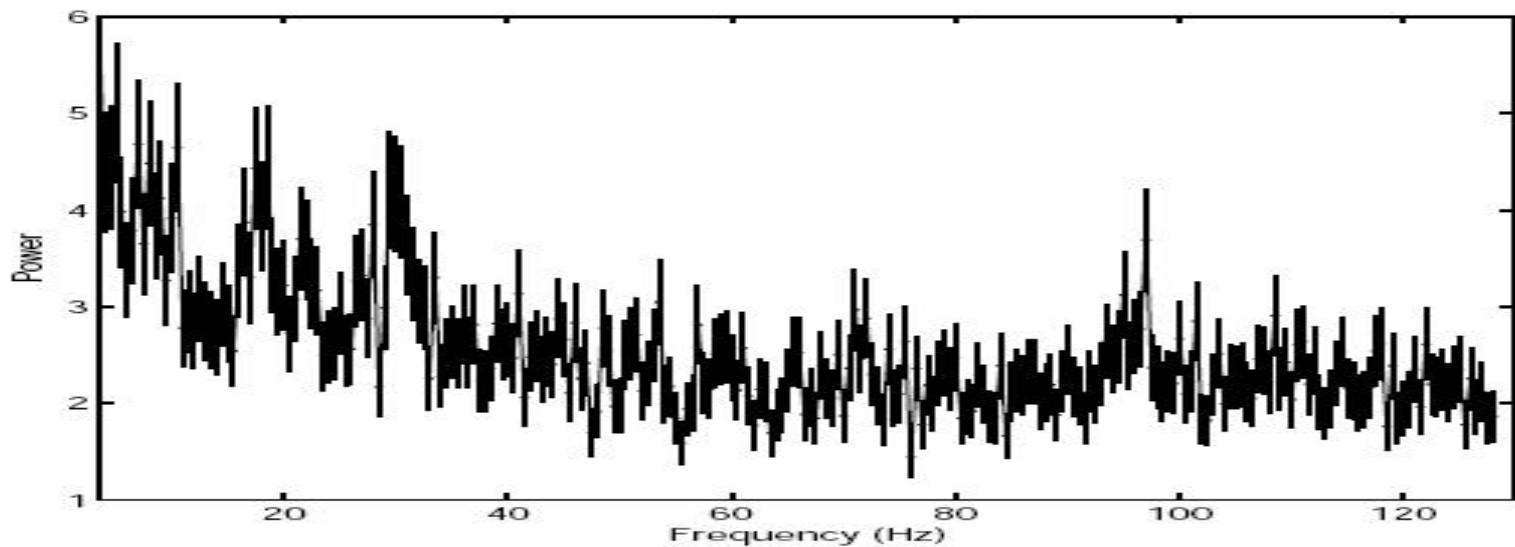
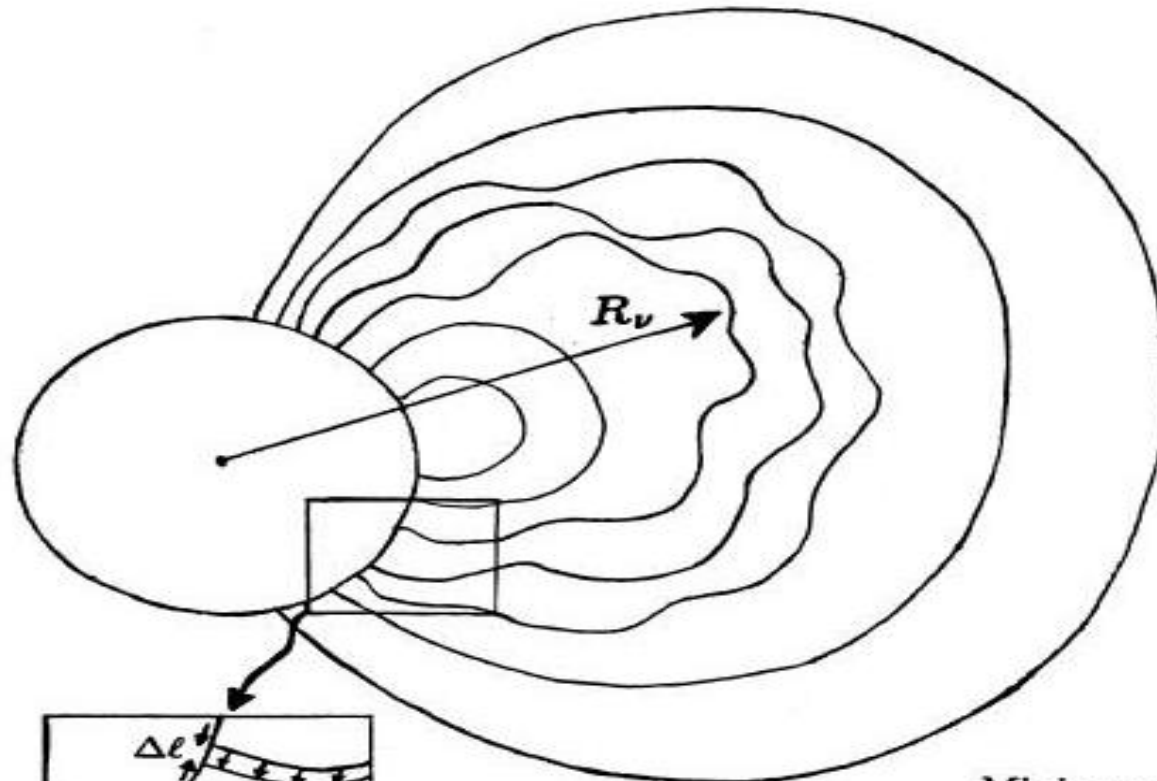


FIG. 3.— Power spectrum accumulated from data in the time interval 200–300 s.

| SGR 1806-20 | SGR 1900+14 | Torsional shear mode identification |
|-------------|-------------|-------------------------------------|
| 18*         |             |                                     |
| 26*         |             |                                     |
| 30*         | 28          | $n = 0, l = 2$                      |
|             | 53          | $n = 0, l = 4$                      |
| 92*         | 84          | $n = 0, l = 6$                      |
| 150         |             | $n = 0, l = 10$                     |
|             | 155         | $n = 0, l = 11$                     |
| 625*        |             | $n = 1$                             |
| 1840        |             | $n = 3$                             |

# Sudden Displacement Sends Pulse Into the Surrounding Magnetosphere

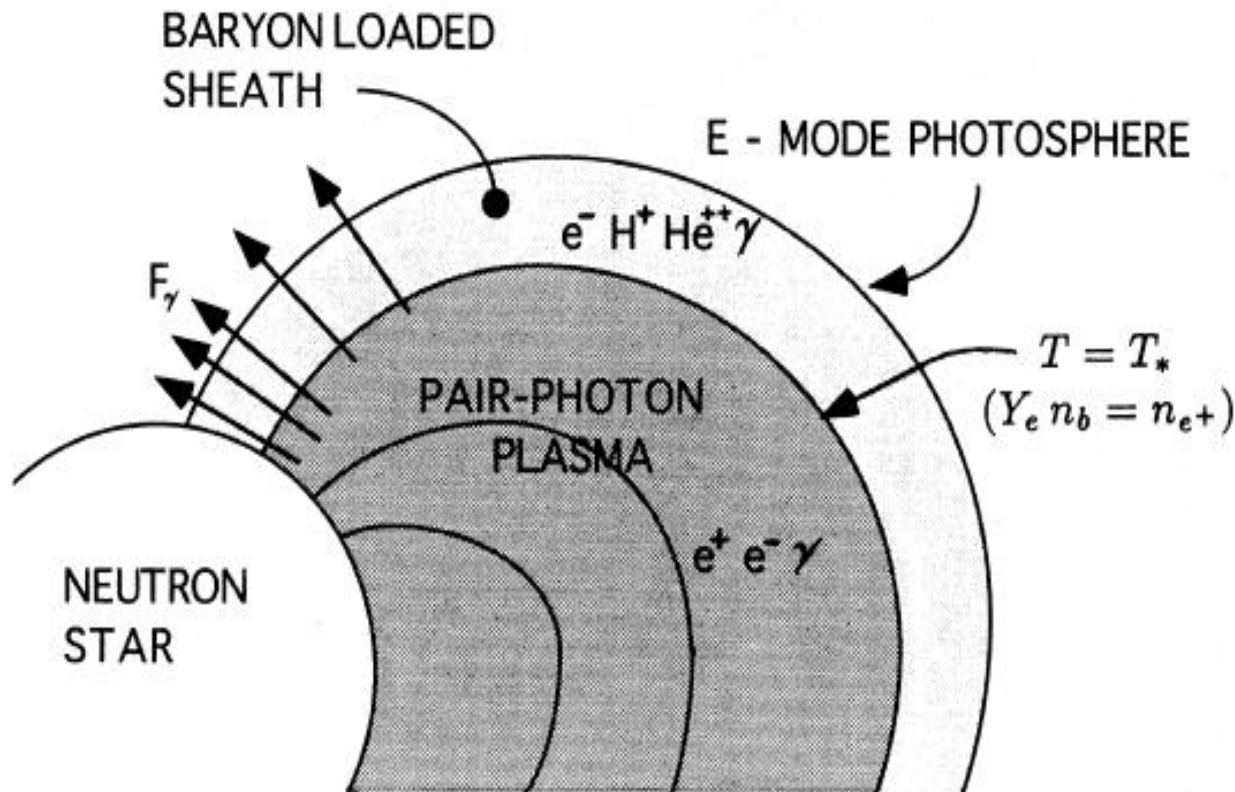


Displacement of  
magnetic footpoints

$$\text{Alfvén excitation frequency} \quad \nu \sim \frac{(\mu/\rho)^{1/2}}{\Delta\ell}$$

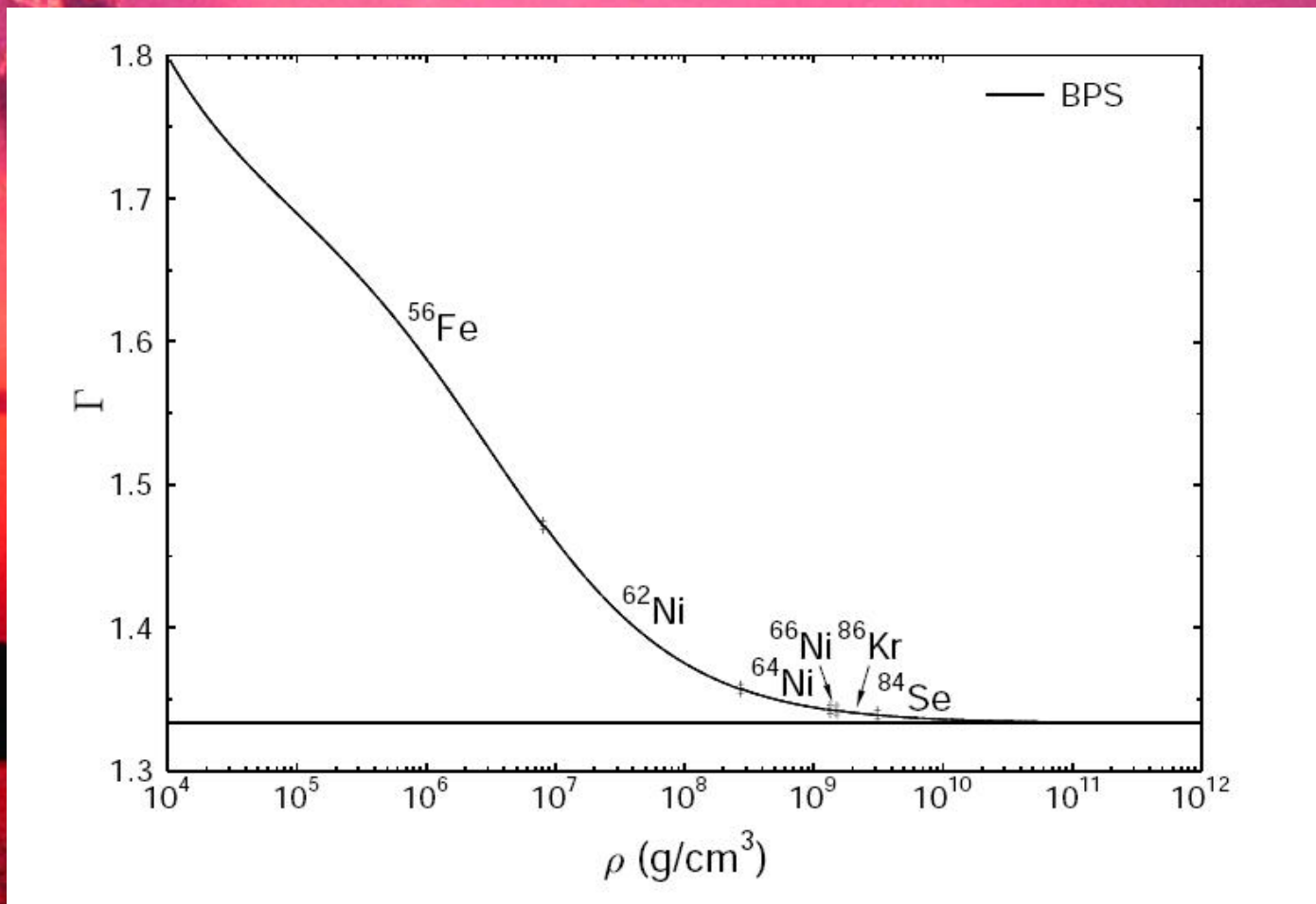
Minimum excitation radius  $R_\nu \sim c/\nu$

# Plasma Generation in Magnetosphere

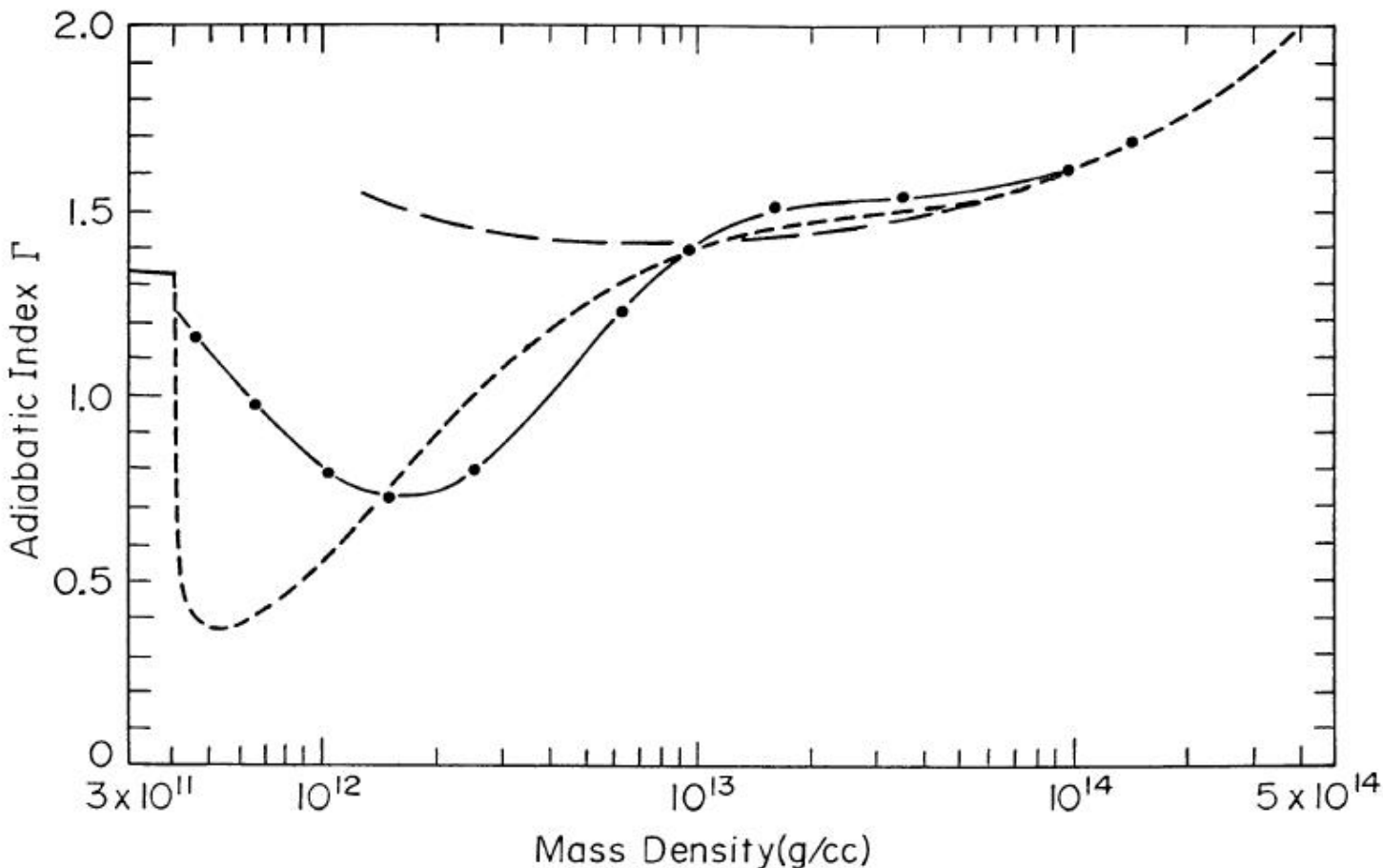


The deposition of  $\geq 10^{38}\text{--}10^{41}$  erg in the magnetosphere of a neutron star is sufficient to generate an optically thick photon-electron-positron plasma. The surface of this plasma is congruent with the magnetic field lines. The surface layers lose heat by radiative diffusion, and the scattering opacity in these layers is dominated by a small contaminant of ions and electrons blown off the neutron star surface.

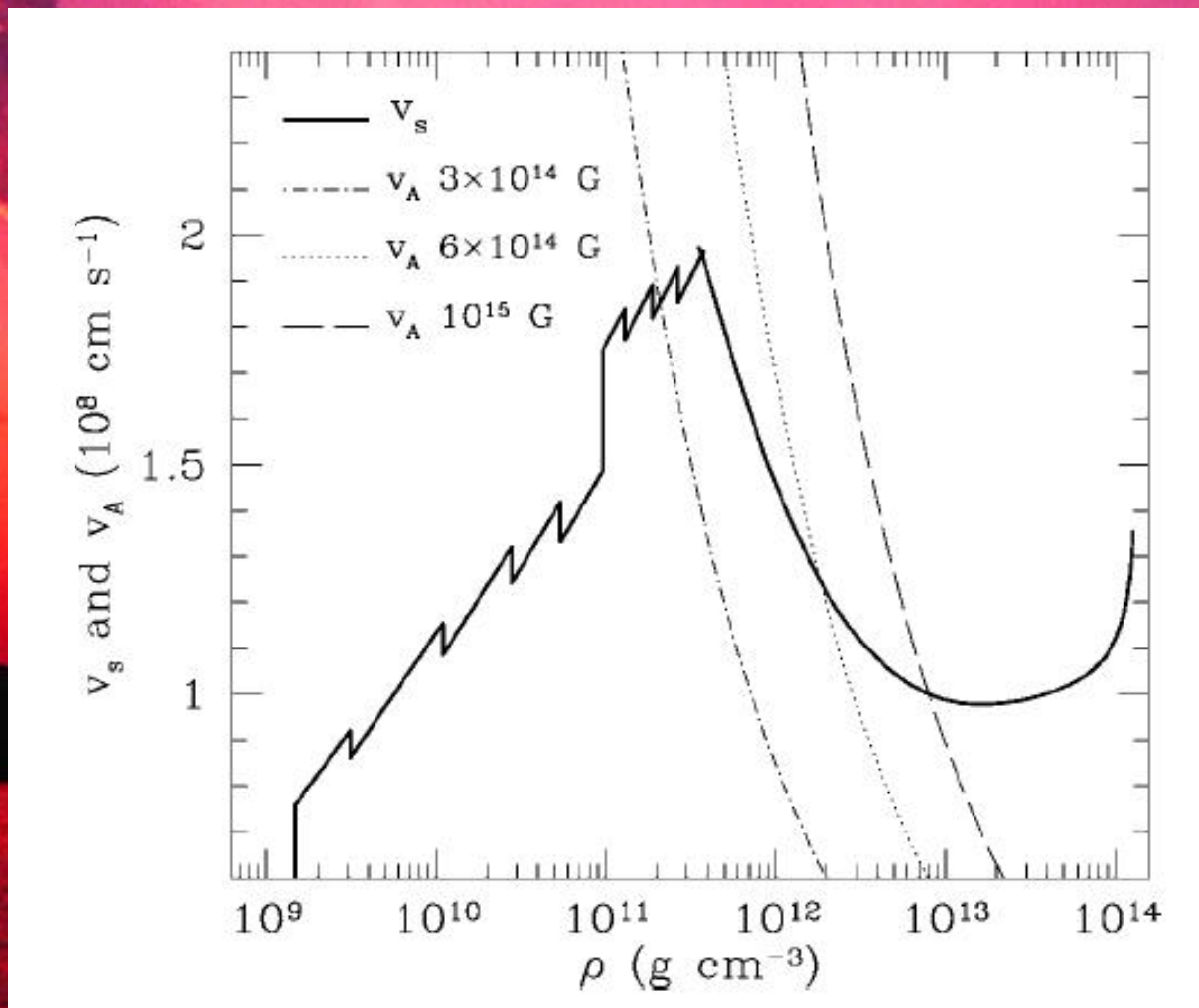
# Adiabatic Indices at Varying Densities Below Neutron Drip



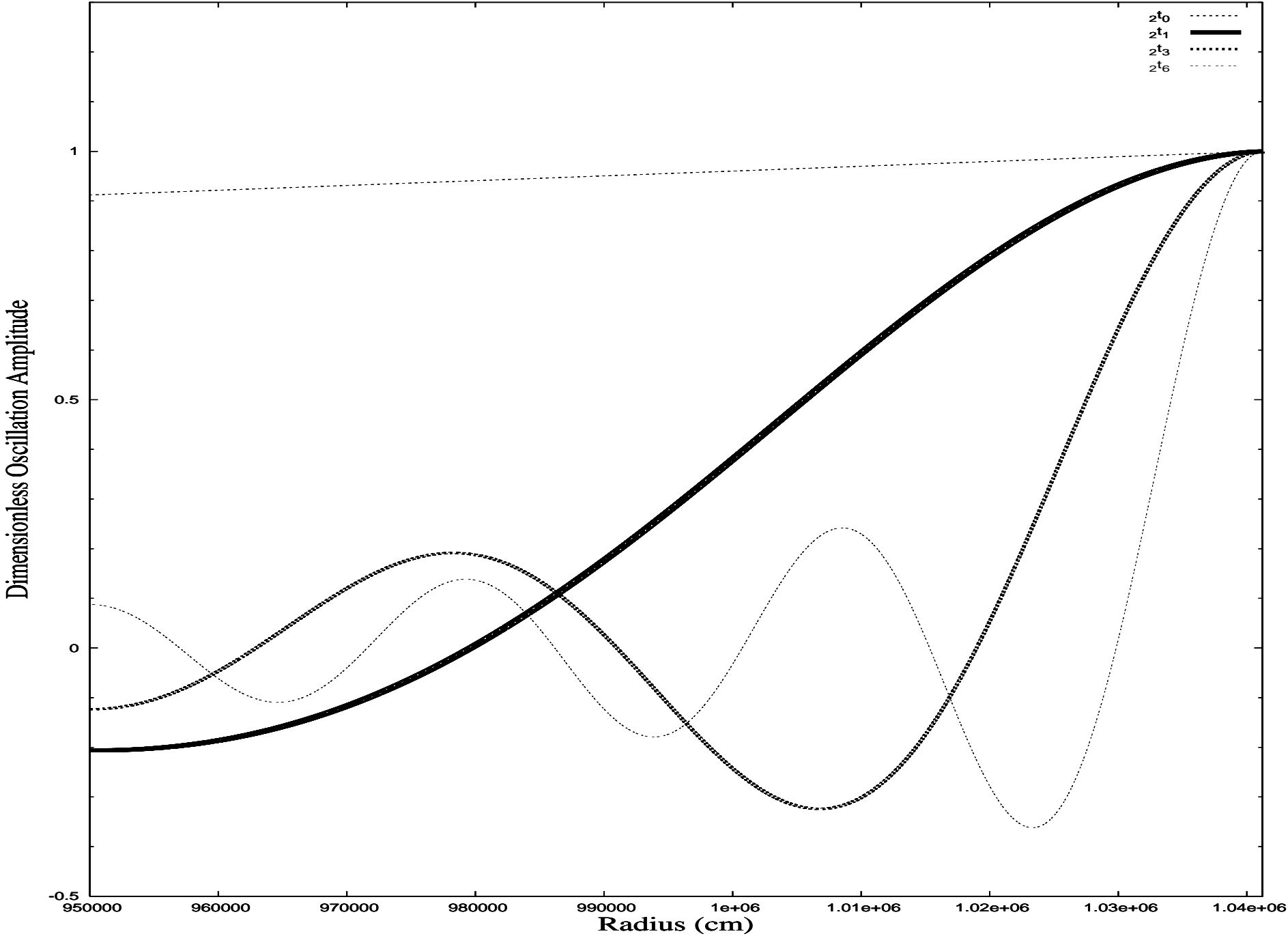
# Adiabatic Indices at Varying Densities Above Neutron Drip



# Shear Speed Nearly Constant Throughout Crust



# Oscillation Amplitudes for l=2: NS 07R95



# NS 11R9

## Toroidal Mode Frequency

- **Thickness:** 8.24%
- **Mass Ratio:** 4.09%
- **Surface Redshift:** ~ 0.27
- **Radius Estimate:** ~ 9km

Toroidal Mode Frequencies of Model NS 11R9 (Hz)

|              | ${}_1t_0$<br><b>Redshifted Frame</b> | ${}_1t_0$<br><b>NS Surface</b> | ${}_1t_1$<br><b>Redshifted Frame</b> | ${}_1t_1$<br><b>NS Surface</b> |
|--------------|--------------------------------------|--------------------------------|--------------------------------------|--------------------------------|
| ${}_1t_n$    | -                                    | -                              | 625.061772                           | 790.591627                     |
| ${}_2t_n$    | 29.674249                            | 37.532631                      | 625.746418                           | 791.457582                     |
| ${}_3t_n$    | 46.918967                            | 59.344123                      | 626.771992                           | 792.754751                     |
| ${}_4t_n$    | 62.948149                            | 79.618178                      | 628.136832                           | 794.481029                     |
| ${}_5t_n$    | 78.509744                            | 99.300820                      | 629.838746                           | 796.633646                     |
| ${}_6t_n$    | 93.836531                            | 118.686471                     | 631.875019                           | 799.209169                     |
| ${}_7t_n$    | 109.027436                           | 137.900255                     | 634.242453                           | 802.203550                     |
| ${}_8t_n$    | 124.132206                           | 157.005094                     | 636.937371                           | 805.612141                     |
| ${}_9t_n$    | 139.178736                           | 176.036271                     | 639.955659                           | 809.429737                     |
| ${}_{10}t_n$ | 154.183923                           | 195.015155                     | 643.292790                           | 813.650612                     |
| ${}_{11}t_n$ | 169.158612                           | 213.955465                     | 646.943856                           | 818.268559                     |
| ${}_{12}t_n$ | 184.110087                           | 232.866414                     | 650.903605                           | 823.276936                     |
|              |                                      |                                |                                      |                                |
|              |                                      |                                |                                      |                                |
|              | ${}_1t_2$<br><b>Redshifted Frame</b> | ${}_1t_2$<br><b>NS Surface</b> | ${}_1t_3$<br><b>Redshifted Frame</b> | ${}_1t_3$<br><b>NS Surface</b> |
| ${}_1t_n$    | 1150.276329                          | 1454.894333                    | 1670.481165                          | 2112.860650                    |
| ${}_2t_n$    | 1150.648802                          | 1455.365452                    | 1670.737735                          | 2113.185165                    |
| ${}_3t_n$    | 1151.207295                          | 1456.071845                    | 1671.122519                          | 2113.671848                    |
| ${}_4t_n$    | 1151.951531                          | 1457.013172                    | 1671.635425                          | 2114.320583                    |
| ${}_5t_n$    | 1152.881155                          | 1458.188980                    | 1672.276338                          | 2115.131224                    |
| ${}_6t_n$    | 1153.995717                          | 1459.598703                    | 1673.045110                          | 2116.103583                    |
| ${}_7t_n$    | 1155.294687                          | 1461.241667                    | 1673.941567                          | 2117.237441                    |
| ${}_8t_n$    | 1156.777442                          | 1463.117089                    | 1674.965501                          | 2118.532535                    |
| ${}_9t_n$    | 1158.443282                          | 1465.224079                    | 1676.116684                          | 2119.988576                    |
| ${}_{10}t_n$ | 1160.291420                          | 1467.561643                    | 1677.394852                          | 2121.605230                    |
| ${}_{11}t_n$ | 1162.320989                          | 1470.128687                    | 1678.799715                          | 2123.382131                    |
| ${}_{12}t_n$ | 1164.531045                          | 1472.924012                    | 1680.330958                          | 2125.318881                    |

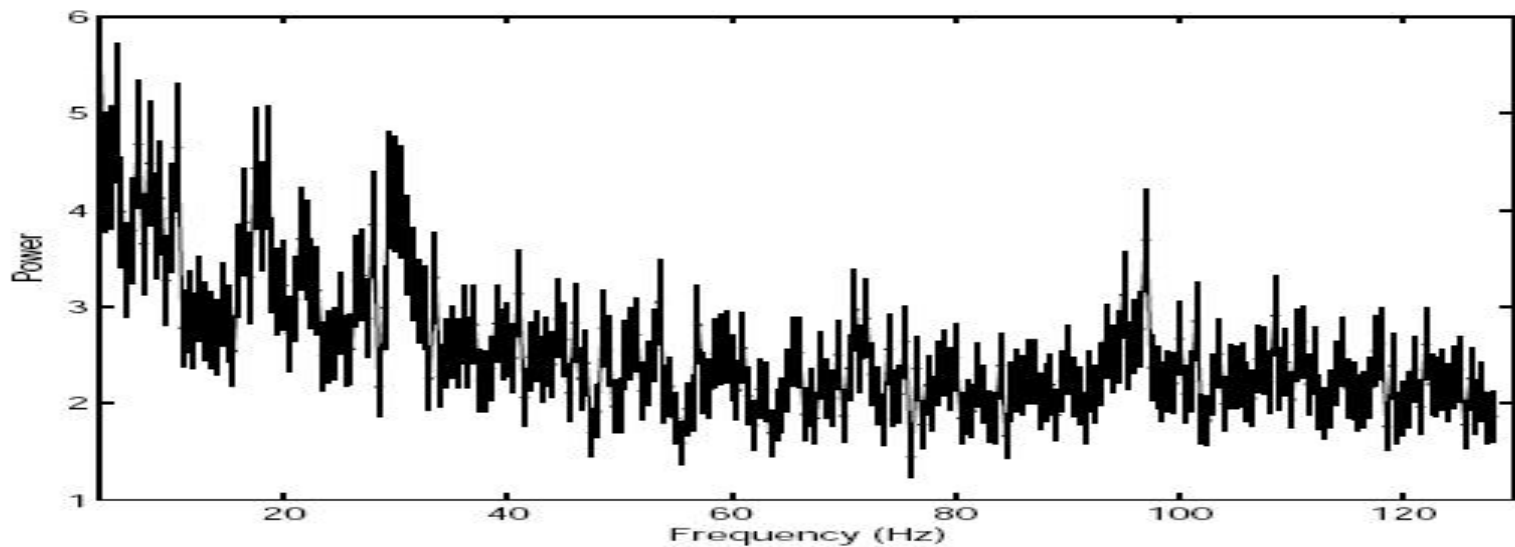


FIG. 3.— Power spectrum accumulated from data in the time interval 200–300 s.

| SGR 1806-20 | SGR 1900+14 | Torsional shear mode identification |
|-------------|-------------|-------------------------------------|
| 18*         |             |                                     |
| 26*         |             |                                     |
| 30*         | 28          | $n = 0, l = 2$                      |
|             | 53          | $n = 0, l = 4$                      |
| 92*         | 84          | $n = 0, l = 6$                      |
| 150         |             | $n = 0, l = 10$                     |
|             | 155         | $n = 0, l = 11$                     |
| 625*        |             | $n = 1$                             |
| 1840        |             | $n = 3$                             |

# NS 24R115

## Toroidal Mode Frequency

- Redshift neglected model yields NS with unrealistically high densities
- Information on crust thickness still informative

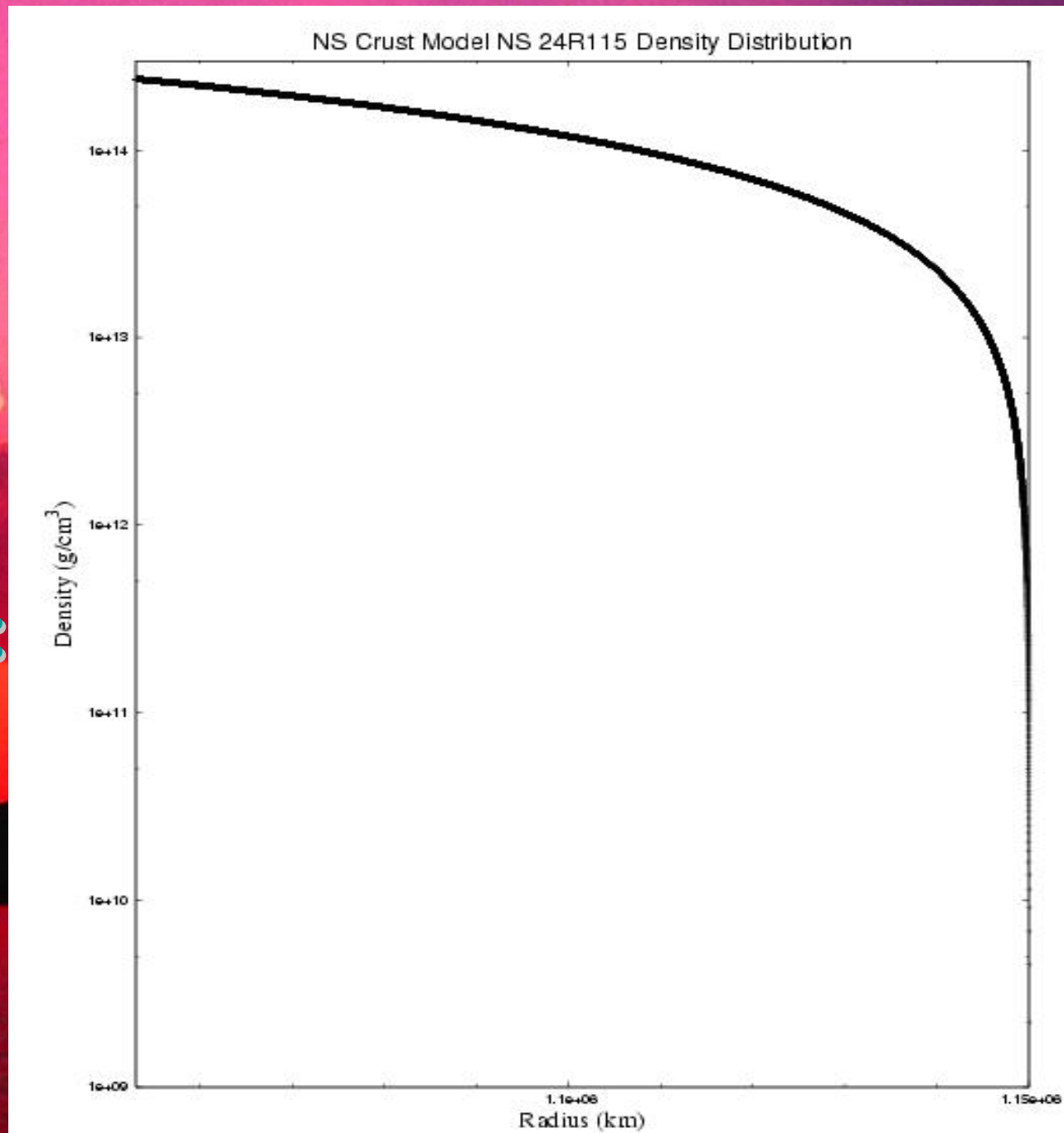
|       | $t_0$      | $t_1$      |
|-------|------------|------------|
| $t_n$ | -          | 623.549219 |
| $t_n$ | 29.308363  | 624.218862 |
| $t_n$ | 46.340456  | 625.221987 |
| $t_n$ | 62.172008  | 626.557002 |
| $t_n$ | 77.541746  | 628.221801 |
| $t_n$ | 92.679580  | 630.213783 |
| $t_n$ | 107.683218 | 632.529872 |
| $t_n$ | 122.601797 | 635.166543 |
| $t_n$ | 137.462867 | 638.119839 |
| $t_n$ | 152.283122 | 641.385414 |
| $t_n$ | 167.073274 | 644.958547 |
| $t_n$ | 181.840518 | 648.834185 |
|       | $t_2$      | $t_3$      |
| $t_n$ | 1147.44418 | 1666.34735 |
| $t_n$ | 1147.80851 | 1666.59831 |
| $t_n$ | 1148.35479 | 1666.97468 |
| $t_n$ | 1149.08276 | 1667.47638 |
| $t_n$ | 1149.99208 | 1668.10329 |
| $t_n$ | 1151.08231 | 1668.85527 |
| $t_n$ | 1152.35295 | 1669.73215 |
| $t_n$ | 1153.80341 | 1670.73374 |
| $t_n$ | 1155.43300 | 1671.85982 |
| $t_n$ | 1157.24097 | 1673.11013 |
| $t_n$ | 1159.22650 | 1674.48439 |
| $t_n$ | 1161.38867 | 1675.98231 |

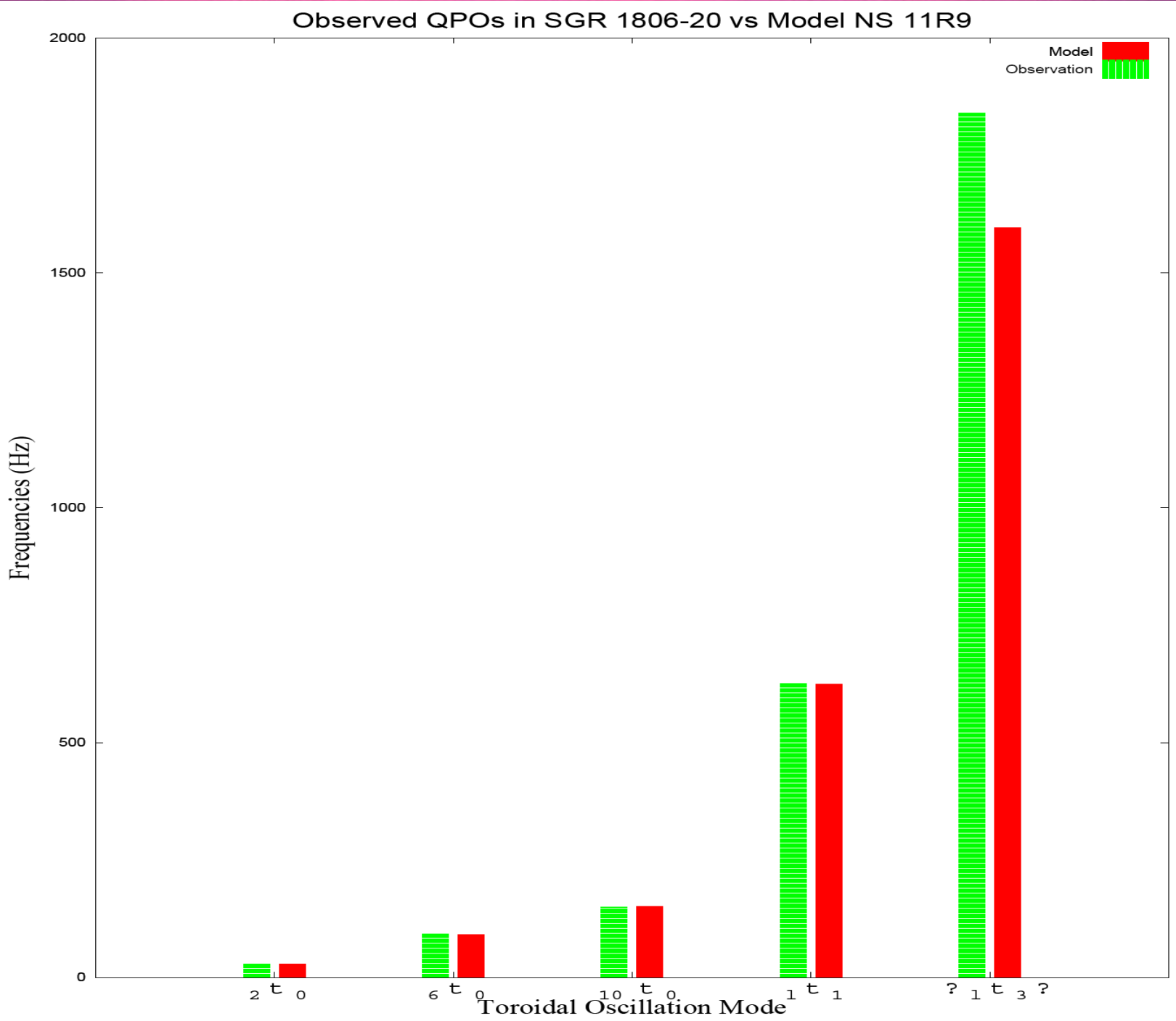
- Thickness:

8.43%

- Mass Ratio:

3.49%





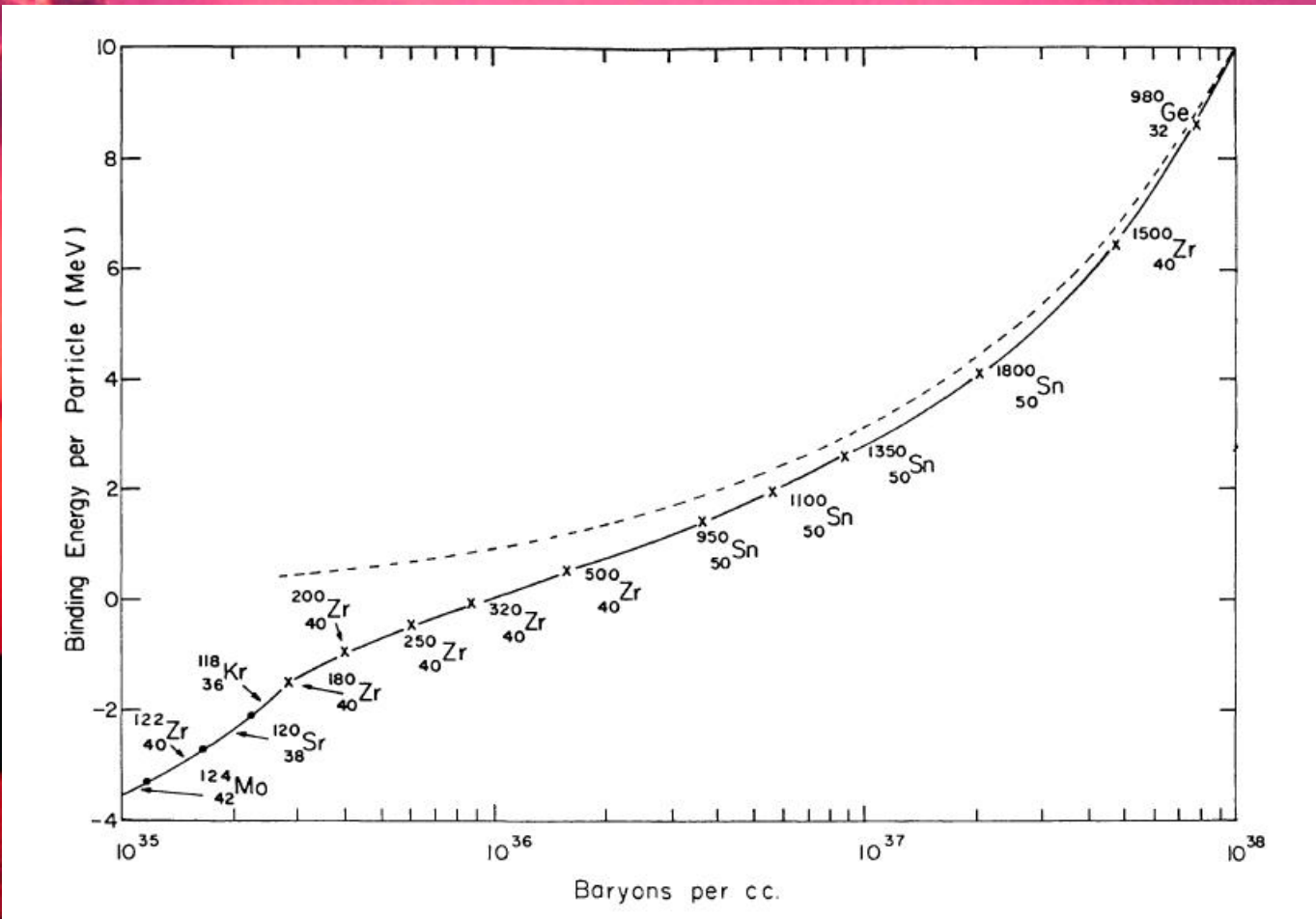
# Some Thoughts

- Crust turned out to be about half as thick as expected
- Would expect that this could be slightly mitigated by adding the effects of the magnetic field into the pulsation equation
- Waiting for more flares!

# References

- Baym, G., Pethick, C., and Sutherland, P. 1971, ApJ. 170, 299.
- Duncan, R.C. 2003, <http://solomon.as.utexas.edu/>.
- Lorenz, C.P., Ravenhall, D.G., and Pethick, C.J. 1993, Phys. Rev. Lett., 70, 4.
- Negele, J.W. 1974, *Physics of Dense Matter*, IAU Symposium 53, Dordrecht, Boston, Reidel, p.1.
- Piro, A. 2005, ApJ, 634, L153.
- Thompson, C. and Duncan, R.C. 1995, Mon. Not. R. Ast. Soc., 275, 255.
- Watts, A. and Strohmayer, T.E. 2007, arXiv:astro-ph/0608476.

# Binding Energy of Extremely Large Nuclei



# Nuclear State Within Neutron Star Crust

